Conjugate Heat Transfer Analysis of a Centrifugal Compressor for Turbocharger Applications

Harald Roclawski, Claus Oberste-Brandenburg, Martin Böhle

Conjugate Heat Transfer Analysis of a Centrifugal Compressor for Turbocharger Applications

Harald Roclawski[1]*, Claus Oberste-Brandenburg[2], Martin Böhle[1]

ISROMAC 2016

International Symposium on Transport Phenomena and Dynamics of Rotating Machinery

Hawaii, Honolulu

April 10-15, 2016

Abstract

For 2-stage turbocharging, high inlet temperatures to the high compressor stage represent an additional load for the compressor wheel which must be taken into account in the design process of the compressor. In this paper, a heat transfer analysis of a high pressure compressor for commercial vehicle applications is presented. Simulations were run with a conjugate heat transfer model. For the simulations, only the compressor side of the turbocharger is modeled. Bearing housing and turbine stage are considered by choosing appropriate thermal boundary conditions at the suitable interfaces. The simulations were validated with experiments run on a gas stand. For the experiments, temperature was measured by means of a telemetry system on 7 locations in the compressor wheel and on the compressor housing. The results are discussed for two operating points with different compressor inlet temperatures.

Keywords

Radial Compressor — CHT Simulation — Turbocharger

[1] *Department of Mechanical Engineering, Technical University of Kaiserslautern, Germany*
[2] *BorgWarner TurboSystems Engineering GmbH, Kirchheimbolanden, Germany*
***Corresponding author**: roclawsk@mv.uni-kl.de

NOMENCLATURE

CFD	Computational Fluid Dynamics
CHT	Conjugate Heat Transfer
CW	Compressor Wheel
c_p	Specific Heat at constant pressure
OP1	Operating Point 1
OP2	Operating Point 2
q	Heat Flux
R	max. Diffuser Radius
R2S	Regulated Two Stage Turbocharging
r	Radius
T	Temperature
T_1	Compressor Inlet Temperature
T_2	Compressor Outlet Temperature
T_t	Total Temperature
TV	Thermocouple Volute
TB	Thermocouple Back Plate
$\dot{V}_{red}$	reduced Volumetric Flow Rate
π	Compressor Pressure Ratio (total-total)
u_2	Compressor tip speed

INTRODUCTION

For many years, turbocharging has been one of the key technologies for achieving high specific power output of internal combustion engines taking also into account more and more stringent emission limits. Additionally, car manufactures attach high importance to a good drivability, which usually is being quantified as a target torque already available at low engine speeds that is fast reached in transient response operation. High specific power output requires high boost pressures. This can be achieved by using a single stage turbocharger but with an unacceptable penalty in transient engine operation [1]. Therefore, for highly downsized engines, regulated 2-stage turbocharging systems (R2S) are applied in order to overcome the conflict of high specific power and simultaneously low specific fuel consumption in agreement with the emission legislation. In case of R2S-systems, two turbochargers of different size are arranged in series. The power of both turbochargers can be regulated by bypass valves and adjusted to the requirements of the combustion engine.

Heat transfer is an important issue for predicting the performance of a turbocharger during the matching process. In general, heat is transferred from the turbine through the bearing housing to the compressor side. Depending on the operating point of the turbocharger, the heat transfer process in the compressor changes. According to [2] at small speeds, heat is transferred to the compressor and only a small amount of heat is transferred through the compressor housing to the ambient. In this case usually the isentropic efficiency of the compressor is calculated too small because of the higher outlet temperature. At high compressor speeds, also heat is transferred to the compressor, but due to the high pressure ratio also a significant amount of heat is transferred to the casing. However the net amount of heat transfer to the compressor is small and thus the effect on compressor performance. The compressor appears to be adiabatic. Besides [2] many researchers investigated the

effect of heat transfer on turbocharger performance numerically and experimentally (e.g. [3],[4]). These investigations are usually performed with single stage compressors with inlet temperatures at ambient conditions. One can expect that the heat transfer mechanism in the compressor differs for the high compressor stage due to the higher inlet temperatures.
Another reason for studying heat transfer in turbochargers is the thermal load of the wheels and casings (e.g. [5] and [6]). Especially in case of R2S turbochargers, for the high-pressure compressor wheel, the load in terms of temperature can be significantly higher than in the single stage case. Therefore it is important to take into account the influence of high compressor wheel temperatures on durability in the design process. In the current paper, a conjugate heat transfer analysis (CHT) for predicting the temperature load on compressor wheels for turbochargers is presented. The results are compared to experimental data obtained under steady state conditions on a gas test stand where the compressor wheel temperatures are measured by means of a telemetry system. The intention of the simulation is to get a deeper understanding of the heat transfer in the high pressure compressor stage, to extend the range of operating points to higher compressor speeds which cannot be covered by the telemetry system and to learn how to create a reliable CHT-model in order to investigate other compressors in the future, where no telemetric measurements are available or possible. The latter one is especially important for passenger car applications where the thermocouples and a telemetry system cannot be installed due to the smaller compressor wheels.

1. METHODS

For the heat transfer analysis, an experimental and numerical approach was chosen. The experiments are necessary to validate the numerical simulations and to provide boundary conditions at the interface between compressor and bearing housing as well as on the ambient surfaces. In the following sections, the experimental setup and the numerical model are described.

1.1 Experimental Setup

For the validation of the CHT analysis, a R2S turbocharger for commercial vehicle applications was mounted on a gas stand test rig. The high pressure compressor was instrumented with thermocouples for measuring the temperatures on the volute, the compressor back plate, the bearing housing and on the compressor wheel. For the compressor wheel, temperature was measured at 7 locations (Figure 1), at the tip of the compressor wheel (CW1), at the fillet of the blades (CW2), at the back side of the wheel (CW3 and CW6), close to the bore of the compressor wheel (CW4 and CW5) and at the shaft (CW7). The position of the thermocouples is given in non-dimensional form for the axial and radial direction. The signals of the thermocouples located in the compressor wheel were transferred via a telemetry system to the data acquisition board. The transmitter of the telemetry system is placed in a sleeve at the end of the shaft at the compressor side (Figure 3). The

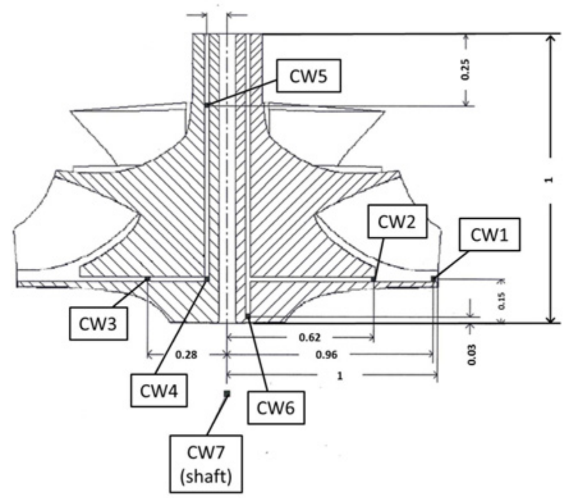

Figure 1. Position of thermocouples on compressor wheel

wiring from the thermocouples to the transmitter is realized through additional holes which are drilled in the compressor wheel. For the measurements, operating points which are typical for the high pressure stage of R2S turbochargers were investigated. Of particular interest are operating points with high wheel temperatures resulting from high compressor inlet temperatures and/or high pressure ratios. The drawback of the telemetry system is that the compressor speed is limited to 140000 rpms. Therefore it is currently not possible to acquire temperature data of the compressor wheel in operating points with high speeds and high temperatures which belong to the most interesting in terms of durability. Another drawback of the telemetry system is the fact, that only 4 signals can be transmitted simultaneously. Therefore two test series were run. In the first case, the signals of the thermocouples 1, 2, 4 and 5 were transmitted, in the second case the signals of the thermocouples 1, 3, 6 and 7. So in order to get a complete test series of all seven thermocouples it s necessary to run each operating point twice. The reproducibility of the tests can be checked by analyzing the operating point (pressure ratio, volumetric flow rate, temperatures at compressor inlet T_1 and outlet T_2) and the signal of thermocouple CW1 which was used in both tests (see Table 1).
The measurement locations on volute casing and back plate are shown in Figure 2. These were used for deriving boundary conditions for the numerical model. In the simulation, a convective boundary condition is applied by specifying the ambient temperature and a heat transfer coefficient. The temperature distribution on casing and back plate can then be calculated and compared to the measurements. In this way, the heat transfer coefficient can be adjusted iteratively until a good agreement with the experimental data is achieved.
In addition, three thermocouples were mounted in the diffuser of the compressor (Figure 3). These were used for validating the calculated gas temperatures.
Figure 4 shows the compressor map of the high speed compressor of the R2S-system. In addition to the R2S operation,

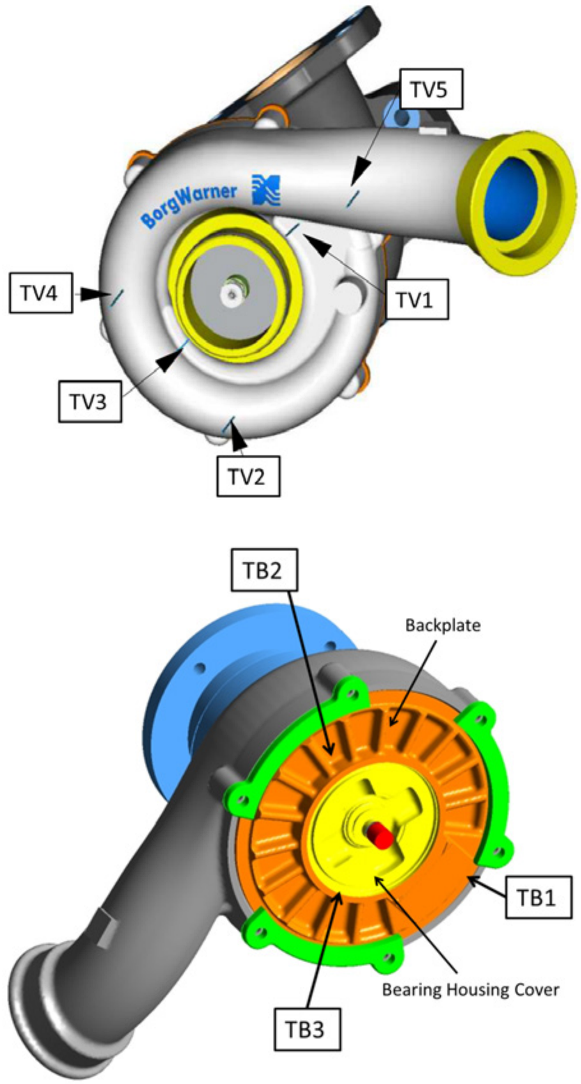

Figure 2. Position of thermocouples on volute and compressor back plate

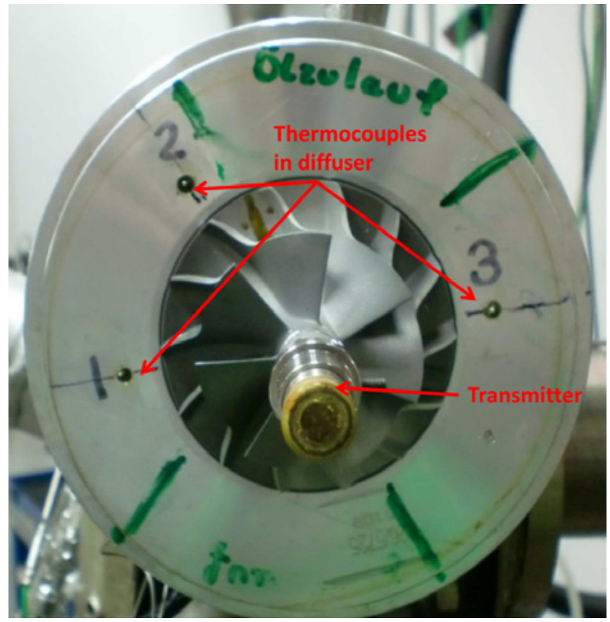

Figure 3. Position of thermocouples in radial diffusor

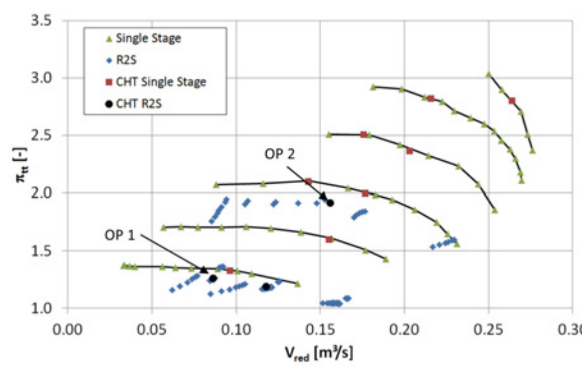

Figure 4. Compressor Map

further tests were run operating the high speed compressor as a single stage compressor. In this way, the difference in wheel temperature between single stage and R2S-system can be analyzed. The operating points where temperatures were measured for the single stage are displayed as green triangles, the R2S operating points are displayed as blue diamonds. Figure 4 also shows the operating points for which, so far, CHT simulations were run. These are displayed as red squares in the single stage case and as black dots for the R2S case.
In this paper, two operating points for the R2S operation are discussed.These are labeled OP1 and OP2 in Figure 4. Table 1 shows the details of both operating points. OP1 was chosen as an operating point with small pressure ratio and volumetric flow rate, but high inlet temperature. In contrast, OP2 has a higher pressure ratio and volumetric flow rate, but a lower inlet temperature. The difference in outlet temperature for both operating points is small. In Section 2 the differences in the heat transfer mechanisms are discussed for both operating points.
As discussed above, two test series were necessary to get the temperature information of all seven thermocouples since the telemetry system can only handle 4 signals at once. Table 1 also shows the signals of thermocouple 1 (T_{CW1}) at the compressor wheel outlet for both tests. A very good reproducibility was achieved in the tests. The difference between both measurements is very small.

1.2 Numerical Model

For the CHT analysis, only the compressor side of the high pressure turbocharger including the piping between the stages was modeled. Figure 5 shows the model for the R2S case. For the single stage calculations, the 180° bend of the inlet piping was replaced by a straight pipe in order to get the same inflow conditions as on the test rig.

All solid parts of the compressor stage were meshed with tetrahedral cells. For the flow domains, hexahedral cells were

Table 1. Operating points for CHT analysis

	OP1	OP2
$\dot{V}_{red}\left[\frac{m^3}{s}\right]$	0.086	0.136
π [-]	1.26	1.91
u_2 [m/s]	235	371
T_1 [K]	405.7	353.8
T_2 [K]	435.7	442.6
$T_{CW1,Test1}$ [K]	420.07	410.68
$T_{CW1,Test2}$ [K]	420.13	410.75

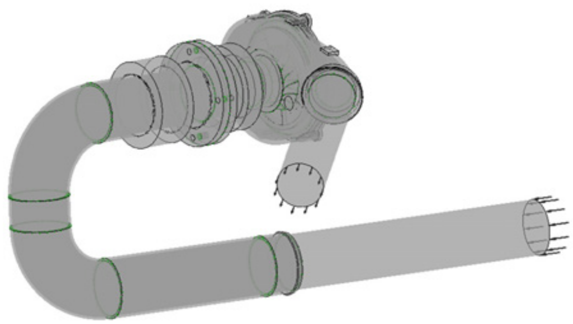

Figure 5. CHT Model of centrifugal compressor

used for all domains except for the volute. The volute was meshed with tetrahedral cells. Prism cells were used to get a good resolution of the boundary layer. In total, the mesh consists of 7,4 Million cells. With this mesh size, y+ values below 15 were realized. In the region of interest, the compressor wheel, the y+ values are below 5. As discussed in Section 2, the comparison of the numerical results to the experimental data shows a very good agreement so that it can be assumed that the mesh is appropriate for the current investigation.
The simulations were run steady state with the software ANSYS CFX using the frozen rotor and the k-ω-SST turbulence model. For modeling the heat transfer between the solid parts in general an ideal contact was assumed and where appropriate, a thermal resistance was specified. In order to get a converged solution about 4000 iteration steps were necessary. The residuals are then below 10^{-4}. To judge convergence, monitors of the compressor pressure ratio and at all locations where temperature was measured were defined. The calculation was considered as converged when the monitors give constant values.
As boundary conditions for the fluid domains, the rotational speed of the compressor wheel was applied to the wheel domain. At the inlet, total pressure and total temperature were specified. At the outlet, the mass flow rate was specified.
Defining the boundary conditions for the solid domains is much more complicated, because there is usually a temperature distribution on the surfaces and not just a constant value. Therefore, a convective boundary condition was used for the volute casing, the compressor back plate and all pipes. In this case, the heat transfer coefficient was chosen based on previous investigations and in the range of natural convection. At the shaft a constant temperature (T_{shaft}) was specified according to the measured temperatures. For the bearing housing, a constant temperature (T_{BH}) was defined according to previous investigations of the heat transfer in turbochargers. For the shaft, the temperature of thermocouple $CW7$ (Figure 1) was used as boundary condition. Heat transfer by radiation is neglected and not included in the model. All other exterior walls of the outlet and inlet pipes were defined as adiabatic.
Figure 6 gives an overview of the applied boundary conditions for the solid domains. For the compressor wheel, the compres-

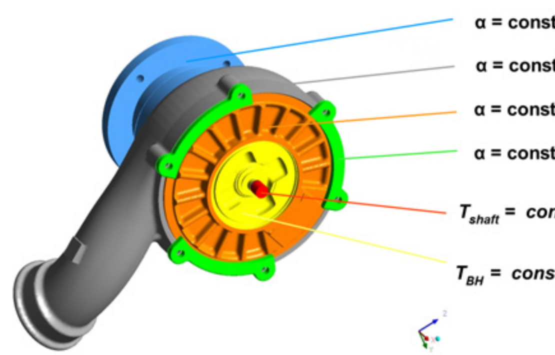

Figure 6. Boundary conditions applied to solid domains

sor housing and the back plate, material properties (density, specific heat capacity and thermal conductivity) of Aluminum were specified. The material properties of steel were used for the shaft and all pipes.

2. RESULTS

In this section, the results of the CHT simulations for OP1 and OP2 are discussed. Table 2 shows the comparison of the calculated and measured operating points for OP1 and OP2. A very good agreement between simulation and experiment was achieved.

Table 2. Accuracy of operating point

	OP1 EXP	OP1 CFD	OP2 EXP	OP2 CFD
$\dot{V}_{red}\left[\frac{m^3}{s}\right]$	0.086	0.086	0.1369	0.1372
π [-]	1.26	1.24	1.91	1.89
u_2 [m/s]	235	235	371	371
T_1 [K]	405.7	405.7	353.8	353.8
T_2 [K]	435.7	438.0	442.6	442.91

A comparison of the measured temperatures to the calculated temperatures of compressor wheel, volute, back plate and diffuser is shown in Table 3. The simulation provides a good match for the measurements of the material temperature. In case of OP2 the thermocouples CW3, CW6 and CW7 were broken and did not produce a result. In the case of OP1, the values for TB1 and TB2 are over-predicted by the simulation. In this case the convective boundary condition does not agree with the experience of the authors and needs to be adjusted for future calculations.

Table 3. Accuracy of temperatures

	OP1 $\Delta T_{EXP} - T_{CFD}[K]$	OP2 $\Delta T_{EXP} - T_{CFD}[K]$
CW1 [K]	-1.6	6.5
CW2 [K]	-5.6	3.7
CW3 [K]	-7.6	-
CW4 [K]	-6.5	5.2
CW5 [K]	-6.3	1.6
CW6 [K]	-5.2	-
CW7 [K]	0	-
TB1 [K]	-10.29	0.3
TB2 [K]	-8.55	0.92
TV1 [K]	-2.35	-1.12
TV2 [K]	-2.44	2.58
TV3 [K]	-2.21	-0.91
TV4 [K]	-2.6	1.53
TV5 [K]	-5.05	0.85

The temperature distribution corresponding to the values in Table 3 on the volute is shown in Figure 7 for both operating points. The temperature increases in radial direction in the diffuser and volute due to the deceleration of the flow. A further increase can be observed in the pressure pipe. As OP2 has a larger pressure ratio and the smaller inlet temperature, the maximum temperature and the temperature increase is higher than for OP1.

Figure 8 shows the temperature distribution on the compressor back plate and the cover of bearing housing. At the bearing housing cover, the temperature is constant as defined by the boundary condition. For the back plate, the temperature increases with radius and is nearly constant in circumferential direction.

The temperature distribution for the compressor wheels is depicted in Figure 9. For both wheels the temperature distribution is uniform in circumferential direction, but there is a gradient in radial direction. For OP1, the temperature increases by approximately $10K$, for OP2 by approximately $30K$. The larger increase in temperature for OP2 is a result of the higher pressure ratio. However, the temperature level is higher in case of OP1 because of the higher inlet temperature

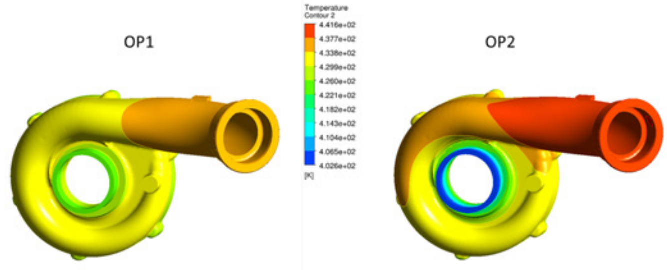

Figure 7. Temperature distribution on volute for OP1 and OP2

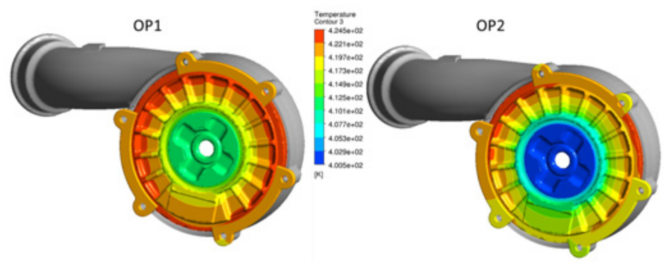

Figure 8. Temperature distribution on back plate for OP1 and OP2

T_1 (see Table 1).

In the following, the heat transfer situation for both operating

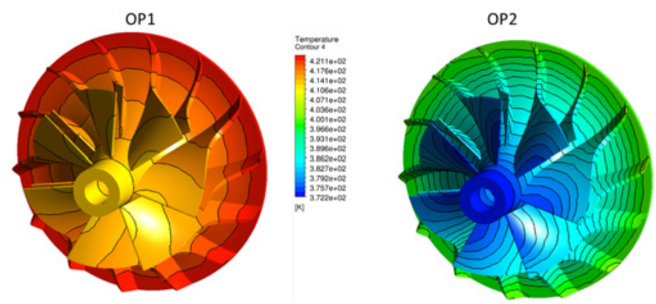

Figure 9. Temperature distribution on compressor wheel

points is discussed. In Table 4, the heat transfer to and from different parts of the compressor wheel is listed. The names of the different parts are defined as in Figure 10. As for the temperature distribution, differences in heat transfer can be observed for both operating points. In case of OP1, heat is added to the compressor wheel at the hub and at the blades. Heat is removed through bore, nut and wheel cavity. So, in this case the compressor wheel is basically heated due to the high inlet temperature.

For OP2, a different heat transfer situation can be observed. Here, almost all heat is added through the wheel cavity and a minor fraction through the shaft. Most of the heat is removed through the blades and also through the hub and nut of the compressor wheel. In contrast to OP1, the heat transfer to the

Table 4. Heat Transfer to compressor wheel

	OP1	OP2
Wheel cavity	-0.22 W	13.42 W
Blades	0.6 W	-13.59 W
Hub	3.24 W	-0.178 W
Bore	-2.92 W	2.37 W
Nut	-0.71 W	-1.96 W

wheel is because of the higher pressure ratio. Due to the higher temperature at compressor wheel outlet, the temperature in the wheel cavity is higher and due to the secondary flow in the cavity, the heat is transferred into the wheel. There is no additional heat transfer from the bearing housing cover (turbine side) in this case, since heat is also transferred from the cavity to the bearing housing cover.

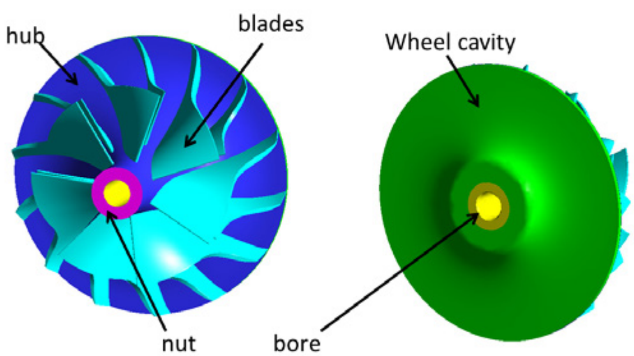

Figure 10. Notation for compressor wheel parts

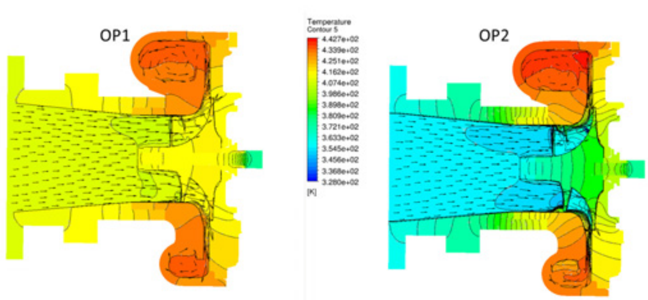

Figure 11. Temperature distribution on compressor cross section

Figure 11 shows the temperature distribution in a cross section of the compressor stage and supports the observation from Table 4. However, the situation is a bit more complicated. Figures 12 and 13 show the heat transfer at the compressor wheel. Red colors indicate a heat transfer to the compressor wheel, blue colors indicate a heat transfer from the compressor wheel. For both operating points heat is rejected from the wheel in the hub region for diameters smaller than about 70% of the wheel tip diameter and at the blades for a span smaller than 80%. Above these limits, heat is transferred to the wheel. Regarding Table 4, the integral values of blade and hub as well as the direction of heat transfer is different for both operating points because of the different magnitude of heat flux. A considerably different situation can be observed at the back of the compressor wheel. In case of OP1 heat is mainly rejected at the back and the bore for the shaft. In contrast, for OP2, it can be seen that heat transfer to the wheel occurs in the wheel cavity and bore.

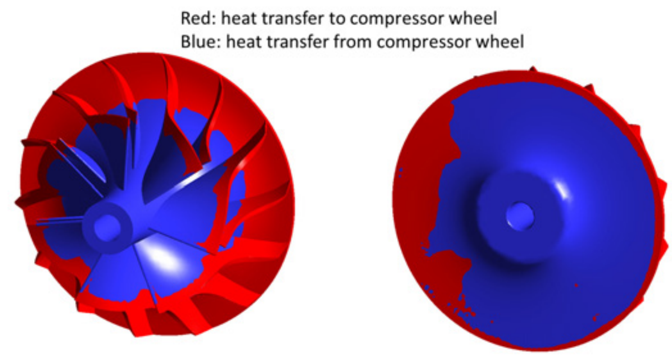

Figure 12. Heatflux of compressor wheel at OP1

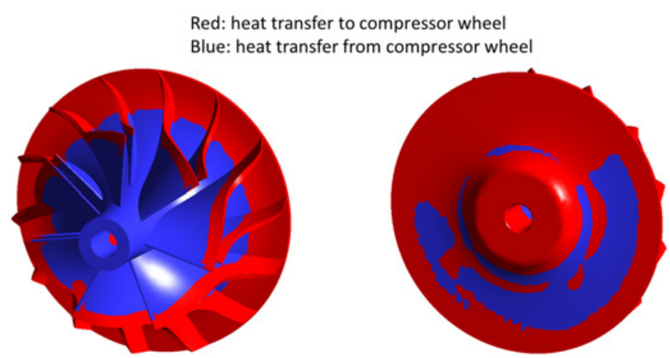

Figure 13. Heatflux of compressor wheel at OP2

In Figure 14 the total temperature distribution in radial direction in the diffuser is shown. The temperature values are averaged in circumferential direction. The total temperature decreases with radius for both operating points. According to the first law of thermodynamics for an open system, the total temperature in the diffuser can be calculated by Equation 1 for the case that there is no work, but heat transfer.

$$T_t = T_t(r/R = 0) + \frac{q}{c_p} \tag{1}$$

Equation 1 shows that the total temperature is decreased when the heat flux becomes negative, e.g. when heat is transferred from the gas to the housing. So also in this case, the simulation provides reasonable results.

In Figure 14, also a comparison with the measured total temperature from the thermocouples located in the diffuser

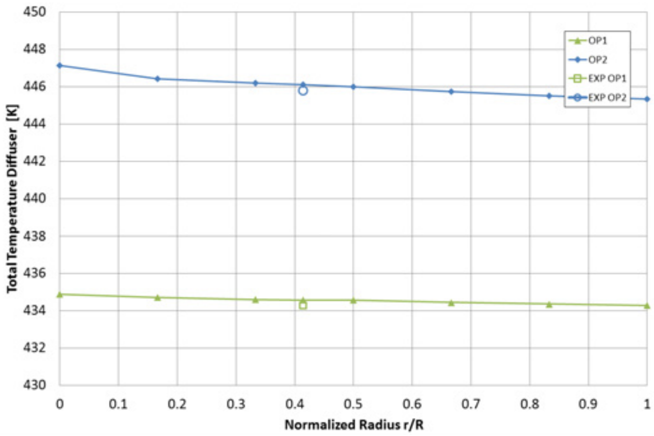

Figure 14. Temperature distribution in radial diffuser

(Figure 3) is shown. The experimental value is the averaged value of the three thermocouples and agrees very good with the numerical simulation.

3. CONCLUSION

A heat transfer study of the high pressure compressor stage of a R2S-turbocharger has been presented. It was shown that with the applied modeling method results with a good accuracy can be achieved. Two operating points of the high pressure compressor have been discussed. It was shown that the heat transfer inside the compressor changes with higher inlet temperature. In case of OP1, the heat transfer to the compressor wheel is mainly due to the high inlet temperature, whereas in case of OP2 the heat transfer to the compressor wheel is caused by the high pressure ratio. This shows that the inlet temperature is also an important parameter especially in the case of R2S-systems and needs to be taken into account in the matching and mechanical design process.
The temperature distribution in the compressor wheel was found to be uniform in circumferential direction. In radial direction, a gradient of 30 K exists for OP2.
In the future, the mesh will be improved to realize smaller y+ values. Also a comparison between 2-stage and single-stage operation of the compressor will be performed. More operating points will be calculated in order to learn how to adapt the boundary conditions on the exterior walls of the compressor on dependency of the operating point. Finally, with these boundary conditions other compressors will be modeled for investigating the effect of wheel diameter and wheel type on the heat transfer in the compressor stage.

REFERENCES

[1] S. Guilain, A. Lefebvre, L. Doleac, G. Schreiber, and Münz. S. Optimization of a small two-stage turbocharged diesel engine. *Aufladetechnische Konferenz*, 2006.

[2] S. Shaaban and J. Seume. Impact of turbocharger non-adiabatic operation on engine volumetric efficiency and tubro lag. *International Journal of Rotating Machinery*, 2012, 2012.

[3] T. Heuer, D. Bohn, and K. Kusterer. Conjugate flow an heat transfer investigation of a turbo charger: Part i: Numerical results. *Proceedings of ASME Turbo Expo 2003 Power for Land Sea and Air*, 2003.

[4] L. Gu, A. Zemp, and S. A. Reza. Numerical study of the heat transfer effect on a centrifugal compressor performance. *Proc IMechE Part C: Journal of Mechanical Engineering Science*, 2014.

[5] C. Oberste-Brandenburg, M. Shogi, M. Gugau, and F Kruse. On the influence of thermal boundary conditions on the thermo mechanical analysis of turbine housing of a turbocharger. *10th International Conference on Turbochargers and Turbocharging*, 2012.

[6] I. Makarenko, B. Lehmayr, M. Bogner, M. Klaus, and M. Singer. Thermomechanical behabiour of turbocharger compressor wheels. *Proceedings of ASME Turbo Expo 2012 Power for Land Sea and Air*, 2012.